On Favorable Bounds on the Spectrum of Discretized Steklov-Poincaré Operator and Applications to Domain Decomposition Methods

Petr Vodstrčil[a], Dalibor Lukáš[a], Zdeněk Dostál[a,b], Marie Sadowská[a]
David Horák[a,c], Oldřich Vlach[a,b], Jiří Bouchala[a], Jakub Kružík[a,c]

[a] Department of Applied Mathematics, FEECS,
VSB - Technical University of Ostrava, Czech Republic

[b] IT4Innovations National Supercomputing Center,
VSB - Technical University of Ostrava, Czech Republic

[c] Institute of Geonics of the Czech Academy of Sciences,
Ostrava, Czech Republic

E-mails: {petr.vodstrcil}{dalibor.lukas}{zdenek.dostal}{marie.sadowska}
{david.horak}{oldrich.vlach2}{jiri.bouchala}{jakub.kruzik}@vsb.cz

October 17, 2023

Abstract

The efficiency of numerical solvers of PDEs depends on the approximation properties of the discretization methods and the conditioning of the resulting linear systems. If applicable, the boundary element methods typically provide better approximation with unknowns limited to the boundary than the Schur complement of the finite element stiffness matrix with respect to the interior variables. Since both matrices correctly approximate the same object, the Steklov-Poincaré operator, it is natural to assume that the matrices corresponding to the same fine boundary discretization are similar. However, this note shows that the distribution of the spectrum of the boundary element stiffness matrix is significantly better conditioned than the finite element Schur complement. The effect of the favorable conditioning of BETI clusters is demonstrated by solving huge problems by H-TBETI-DP and H-TFETI-DP.

1 Introduction

The finite element (FEM) and boundary element method (BEM) are two fundamental methods for discretizing elliptic boundary value problems. Here, we are

interested in their application in the context of un-preconditioned FETI (finite element tearing and interconnecting) and BETI (boundary element tearing and interconnecting) domain decomposition methods for solving huge linear systems arising from the discretization of linear elliptic partial differential equations.

Let us recall that FETI was introduced by Farhat and Roux [1, 2] in the early nineties. The basic idea of FETI is to decompose the domain into subdomains interconnected by Lagrange multipliers, eliminate the primal variables, and get a small dual problem with many reasonably conditioned local problems solvable in parallel. Later achievements include the proof of scalability of FETI [3] by Farhat, Mandel, and Roux and a modification of FETI called FETI-DP (dual-primal) by Farhat, Lesoinne, and Pierson [4] that enforces some constraints on the primal level. More on FETI methods for linear systems and their preconditioning can be found, e.g., in the books by Toselli and Widlund [5] or Pechstein [6].

The local problems are defined by the Schur complements S^i_{FEM} of the subdomains' stiffness matrices with respect to the subdomains' boundaries. The regular condition numbers of S^i_{FEM} are proportional to H/h, where H and h denote the subdomain's diameter and the discretization parameter, respectively. The Schur complements S^i_{FEM} can be considered as a discrete approximation of the Steklov-Poincaré operator mapping the Dirichlet data onto the Neumann data. Alternatively, the approximation S^i_{BEM} of the Steklov-Poincaré operator can be obtained by BEM as proposed by Langer and Steinbach [7] in their paper introducing BETI. Since S^i_{BEM} is obtained by the exact elimination of the unknown interior data and following boundary discretization, it is natural to assume that S^i_{BEM} provides a better approximation to the Steklov-Poincaré operator than S^i_{FEM}. This is of special importance for solving huge inequality-constrained problems such as those arising from the discretization of elliptic variational inequalities. The reason is that the duality transforms the general inequality constraints into bound constraints that can be solved very efficiently by the specialized algorithms, but the standard preconditioners transform the variables and do not preserve the bound constraints.

Since S^i_{FEM} and S^i_{BEM} are the approximations of the same operator, it is natural to assume that they are very similar to each other. Qualitatively, it is true, as the condition numbers of both matrices are proportional to H/h, where H and h denote the diameter of the subdomain and the discretization parameter, respectively. However, closer inspection of the conditioning of S^i_{BEM} is more favorable than that of S^i_{FEM}. The point of this paper is to prove that for a 2D model scalar problem, the regular condition number $\overline{\kappa}(S^i_{\mathrm{BEM}})$ is almost less than half of that of $\overline{\kappa}(S^i_{\mathrm{FEM}})$ for $h \to 0$.

The effect of nice conditioning of the BETI Schur's complements is illustrated on solving large discretized linear problems by the H-TFETI-DP (hybrid-total) method proposed by Klawonn and Rheinbach [8], who used the FETI-DP methodology to interconnect the groups of adjacent subdomains into *clusters* so that the rigid modes' dimension of each cluster and any of its subdomains is the same. With the Dirichlet preconditioner, the resulting hybrid FETI-DP method enjoys a small coarse grid and similar convergence properties as

the original FETI and FETI-DP (see Klawonn and Rheinbach [9], Klawonn et al. [10], and Jungho Lee [11, 12]). The latter author used a variant of FETI called TFETI (total FETI) that enforces the Dirichlet conditions by Lagrange multipliers [13] so that all subdomains are floating. As a result, their stiffness matrices have a priori known kernels and can be reliably inverted, see, e.g., [14, 15]. Most recently, it was proved that the regular condition number of the scalar clusters joined by the interiors of edge [16] or face [17] averages (in the case of elasticity by the rigid body modes of edges [18] or faces [19]) is bounded by a constant multiple of $H/(hm)$, where m denotes a number of subdomains in the cluster in one direction. More on the un-preconditioned H-TFETI method for scalar problems can be found in [20].

We organized the paper as follows. After this introduction, we describe the model problem and review the FETI domain decomposition to the extent sufficient for the rest of our paper. The most important results, including the bounds on the relations between extreme eigenvalues of the Schur complements and the discretized Steklov-Poincaré operators, are in Sect. 3. The estimates are confronted with the results of numerical experiments in Sect. 4. The solution of huge variational equalities discretized by FETI and BETI indicates the strong potential of BETI for solving huge problems.

2 Model Problem and Domain Decomposition

We reduce our presentation to the following model problem, though our reasoning remains valid also for more general cases. Let us consider an elliptic problem governed by the Laplacian on the unit square $\Omega := (0,1)^2 \subset \mathbb{R}^2$ with the boundary $\Gamma := \partial\Omega$, such as the Poisson equation

$$-\triangle u = f \quad \text{on } \Omega \tag{1}$$

together with the Dirichlet and Neumann boundary conditions defined on Γ_D and Γ_N, respectively; $\Gamma_N := \Gamma \setminus \Gamma_D$ with $\Gamma_D \subset \Gamma$ of a non-zero measure. We assume that the known Dirichlet data are homogeneous and u and f are smooth enough, the same as the known Neumann data. For the application of TBETI, let us decompose Ω into square subdomains Ω^i of the equal side-length H with the boundaries $\Gamma^i := \partial\Omega^i$ as in Fig. 1, $i = 1, \ldots, s$, $s := 1/H^2$. Further, let each Γ^i be discretized into non-overlapping line segments of the same length h. We assume a matching discretization of subdomains so the nodes coincide on the interface. For each subdomain's boundary Γ^i, $i = 1, \ldots, s$, we introduce standard boundary element linear and constant basis functions φ^i_j and ψ^i_j to approximate Dirichlet and Neumann data, respectively, and to assemble local discrete Steklov-Poincaré operators S^i, local right-hand sides $\mathbf{f}^i$,

$$\mathsf{S} := \operatorname{diag}(\mathsf{S}^1, \ldots, \mathsf{S}^s), \quad \mathbf{u} := \begin{bmatrix} \mathbf{u}^1 \\ \vdots \\ \mathbf{u}^s \end{bmatrix}, \quad \mathbf{f} := \begin{bmatrix} \mathbf{f}^1 \\ \vdots \\ \mathbf{f}^s \end{bmatrix}.$$

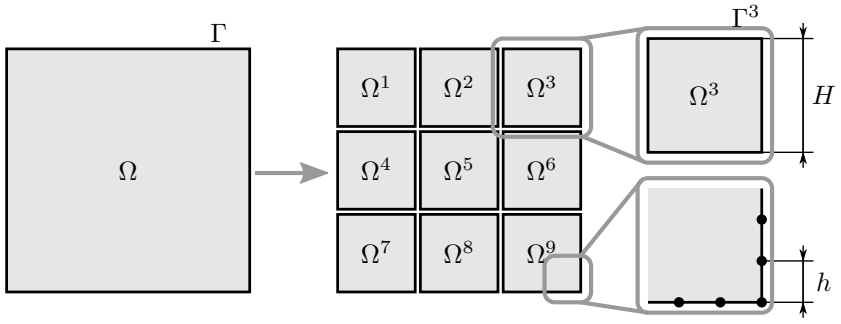

Figure 1: Decomposition of Ω into 3×3 subdomains.

The basis functions φ_j^i span the space V_h^i for the Dirichlet data approximation with the elements

$$u_h^i(x) = \sum_j u_j^i \varphi_j^i(x), \quad x \in \Gamma^i, \quad [\mathbf{u}^i]_j = u_j^i.$$

The global matrix S represents the discrete approximate Steklov-Poincaré operator and is closely related to the Schur complement of the global TFETI stiffness matrix [7]. The matrix S is symmetric positive semidefinite (SPS), with the dense blocks S^i, the kernels of which are spanned by the vector of the appropriate number of ones

$$\mathbf{r}^i := [1, \ldots, 1]^\top.$$

A comprehensive presentation of the boundary integral operators and their properties can be found, e.g., in the book of Steinbach [23].

The solution of discretized problem (1) can be obtained by solving the following equality-constrained quadratic programming problem

$$\min \frac{1}{2}\mathbf{u}^\top \mathsf{S}\mathbf{u} - \mathbf{f}^\top \mathbf{u} \quad \text{w.r.t.} \quad \mathsf{B}\mathbf{u} = \mathbf{o}, \tag{2}$$

where B represents the interconnectivity of subdomains and the Dirichlet boundary conditions, and $\mathbf{o}$ denotes a zero vector. The matrix B has the column blocks complying with the block structure of S, i.e.,

$$\mathsf{B} = [\mathsf{B}^1, \ldots, \mathsf{B}^s]$$

referring for more details on how to construct B to [5].

After applying the standard procedure, see, e.g., [24, 26], including the use of the duality principle and introducing the orthogonal projectors P and Q, we arrive at the TBETI problem

$$\min \frac{1}{2}\boldsymbol{\lambda}^\top \mathsf{PFP}\boldsymbol{\lambda} - \boldsymbol{\lambda}^\top \mathsf{P}\mathbf{d} \tag{3}$$

with

$$\mathsf{P} := \mathsf{I} - \mathsf{Q}, \quad \mathsf{Q} := \mathsf{G}^\top \mathsf{G},$$

$$\mathsf{G} := \mathsf{T}\widetilde{\mathsf{G}}, \quad \widetilde{\mathsf{G}} := \mathsf{R}^\top \mathsf{B}^\top, \quad \mathsf{R} := \mathrm{diag}\,(\mathbf{r}^1, \ldots, \mathbf{r}^s),$$

$$\mathsf{F} := \mathsf{B}\mathsf{S}^+\mathsf{B}^\top, \quad \mathbf{d} := \mathsf{B}\mathsf{S}^+\mathbf{f} - \mathsf{F}\widetilde{\boldsymbol{\lambda}}, \quad \mathsf{S}^+ \text{ being a generalized inverse of } \mathsf{S}.$$

Note that I stands for the identity matrix. The matrix T defines orthonormalization of the rows of $\widetilde{\mathsf{G}}$, so that $\mathsf{G}\mathsf{G}^\top = \mathsf{I}$. The vector $\widetilde{\boldsymbol{\lambda}}$ satisfies $\mathsf{G}\widetilde{\boldsymbol{\lambda}} = \mathsf{T}\mathsf{R}^\top \mathbf{f}$. The columns of R span the kernel of S. The matrices P and Q are the orthogonal projectors on the kernel of G and the image space of $\mathsf{G}^\top$, respectively. The vector $\boldsymbol{\lambda}$ represents Lagrange multipliers corresponding to the equality constraints and

$$\mathsf{S}^+ := \mathrm{diag}\,((\mathsf{S}^1)^+, \ldots, (\mathsf{S}^s)^+)$$

with $(\mathsf{S}^i)^+$ satisfying $\mathsf{S}^i = \mathsf{S}^i(\mathsf{S}^i)^+\mathsf{S}^i$.

Once the solution $\overline{\boldsymbol{\lambda}}$ of (3) is obtained, the primal solution of (2) can be reconstructed via [26]

$$\mathbf{u} = \mathsf{S}^+(\mathbf{f} - \mathsf{B}^\top(\overline{\boldsymbol{\lambda}} + \widetilde{\boldsymbol{\lambda}})) + \mathsf{R}\boldsymbol{\alpha}, \quad \boldsymbol{\alpha} := (\widetilde{\mathsf{G}}\widetilde{\mathsf{G}}^\top)^{-1}\widetilde{\mathsf{G}}(\mathsf{F}\overline{\boldsymbol{\lambda}} - \mathbf{d}).$$

A more effective procedure can also be found in [26].

3 Spectral Analysis

We shall analyze the spectral bounds of the FEM/BEM discretizations of the Steklov-Poincaré operator on a single subdomain, as the bounds coincide with those of the global FETI/BETI Hessian. For the sake of simplicity, we skip the subdomain index, i.e., $\Omega^i \equiv \Omega$, $\Gamma^i \equiv \Gamma$.

Let $\Omega := (0, H)^2 \subset \mathbb{R}^2$ with $H > 0$. We consider an equidistant nonoverlapping discretization of the boundary $\Gamma := \partial\Omega$ into n open segments γ_i that connect nodes $x_{i-1}, x_i \in \Gamma$, $i \in \{1, 2, \ldots, n\}$,

$$\Gamma = \bigcup_{i=1}^{n} \overline{\gamma_i}, \quad \gamma_i \cap \gamma_j = \emptyset \text{ for } i \neq j, \tag{4}$$

where $h = |\gamma_i|$, the length of γ_i, is the discretization step. We assume $x_0 = x_n$. Further, we introduce the boundary element space

$$V^h := \left\{ v^h \in C(\Gamma, \mathbb{R}) \,:\, v^h|_{\gamma_i} \text{ is linear for each } i \in \{1, \ldots, n\},\ \int_\Gamma v^h \, ds = 0 \right\}.$$

We consider a Sobolev space $\widetilde{U} := \{\widetilde{u} \in H^1(\Omega) : \int_\Gamma \widetilde{u}\, ds = 0\}$. By the Poincaré inequality, the latter is equipped with the inner product

$$(\widetilde{u}, \widetilde{v}) := \int_\Omega \nabla\widetilde{u} \cdot \nabla\widetilde{v}\, dx$$

and forms a Hilbert space. Let $\widetilde{U}^h := \{\widetilde{u}^h \in \widetilde{U} : \ \widetilde{u}^h|_\Gamma \in V^h\}$. We consider a regular finite element discretization of Ω into right-angled triangles, see Fig. 2, such that it aligns with the boundary discretization (4). Here, let us note that in what follows, our reasoning is independent of how the squares are divided into two triangles. We shall denote by $\widetilde{V}^h$ the corresponding finite element subspace of $\widetilde{U}^h$ consisting of continuous functions $\widetilde{v}^h : \overline{\Omega} \to \mathbb{R}$ that are piecewise linear over the finite element triangulation.

The analysis aims to compare the spectral bounds of the Steklov-Poincaré operator S discretized by FEM and BEM. The Steklov-Poincaré operator $S : H^{1/2}(\Gamma) \to H^{-1/2}(\Gamma)$ reads as follows:

$$\langle S(u), v\rangle := \int_\Omega \nabla\mathcal{H}(u) \cdot \nabla\mathcal{H}(v)\, dx,$$

where $\mathcal{H} : H^{1/2}(\Gamma) \to H^1(\Omega)$ is the harmonic extension operator defined as the unique solution to the Dirichlet boundary value problem for the Laplace operator, the weak formulation of which reads

$$\begin{cases} \text{Find } \mathcal{H}(u) := \widetilde{u} \in H^1(\Omega) : \ \widetilde{u} = u \text{ on } \Gamma \text{ and} \\ \displaystyle\int_\Omega \nabla\widetilde{u} \cdot \nabla\widetilde{v}\, dx = 0 \quad \forall \widetilde{v} \in H^1_0(\Omega). \end{cases} \tag{5}$$

The finite element discretization of the harmonic extension, restricted to the zero-boundary-mean functions, i.e., $\mathcal{H}^h : V^h \to \widetilde{V}^h$ reads

$$\begin{cases} \text{Find } \mathcal{H}^h(u^h) := \widetilde{u}^h \in \widetilde{V}^h : \ \widetilde{u}^h = u^h \text{ on } \Gamma \text{ and} \\ \displaystyle\int_\Omega \nabla\widetilde{u}^h \cdot \nabla\widetilde{v}^h\, dx = 0 \quad \forall \widetilde{v}^h \in \widetilde{V}^h \cap H^1_0(\Omega). \end{cases}$$

Hence, the Steklov-Poincaré operator $S^h_{\mathrm{FEM}} : V^h \to (V^h)^*$ discretized by FEM is as follows:

$$\langle S^h_{\mathrm{FEM}}(u^h), v^h\rangle := \int_\Omega \nabla\mathcal{H}^h(u^h) \cdot \nabla\mathcal{H}^h(v^h)\, dx. \tag{6}$$

The latter will be compared to the boundary element counterpart $S^h_{\mathrm{BEM}} : V^h \to (V^h)^*$, which reads

$$\langle S^h_{\mathrm{BEM}}(u^h), v^h\rangle := \int_\Omega \nabla\mathcal{H}(u^h) \cdot \nabla\mathcal{H}(v^h)\, dx. \tag{7}$$

We shall later comment on a numerical realization of S^h_{BEM} and an additional approximation error.

In the following subsections, we shall prove that the effective condition number of S^h_{BEM} is asymptotically at least almost half the effective condition number of S^h_{FEM}, namely,

$$\frac{\overline{\kappa}\left(\mathsf{S}^h_{\mathrm{FEM}}\right)}{\overline{\kappa}\left(\mathsf{S}^h_{\mathrm{BEM}}\right)} = \frac{\lambda^h_{\mathrm{BEM}}}{\lambda^h_{\mathrm{FEM}}} \cdot \frac{\Lambda^h_{\mathrm{FEM}}}{\Lambda^h_{\mathrm{BEM}}} \geq c(h) \to \frac{32}{17} \doteq 1.88 \quad \text{as } h \to 0. \tag{8}$$

By the variational principle, the spectral bounds, with respect to a scaled Euclidean inner product $(u^h, v^h)_{h,\Gamma} := h \sum_{i=1}^n u^h(x_i)\, v^h(x_i)$, are defined as

$$\lambda^h_{\mathrm{FEM}} := \min_{v^h \in V^h \setminus \{0\}} \frac{\langle S^h_{\mathrm{FEM}}(v^h), v^h \rangle}{h \sum_{i=1}^n \left[v^h(x_i)\right]^2}, \quad \Lambda^h_{\mathrm{FEM}} := \max_{v^h \in V^h \setminus \{0\}} \frac{\langle S^h_{\mathrm{FEM}}(v^h), v^h \rangle}{h \sum_{i=1}^n \left[v^h(x_i)\right]^2}$$

and

$$\lambda^h_{\mathrm{BEM}} := \min_{v^h \in V^h \setminus \{0\}} \frac{\langle S^h_{\mathrm{BEM}}(v^h), v^h \rangle}{h \sum_{i=1}^n \left[v^h(x_i)\right]^2}, \quad \Lambda^h_{\mathrm{BEM}} := \max_{v^h \in V^h \setminus \{0\}} \frac{\langle S^h_{\mathrm{BEM}}(v^h), v^h \rangle}{h \sum_{i=1}^n \left[v^h(x_i)\right]^2}.$$

3.1 Lower Bounds

We shall prove that the factor $\frac{\lambda^h_{\mathrm{BEM}}}{\lambda^h_{\mathrm{FEM}}}$ in (8) tends to 1. We start with proving this property with respect to the $L^2(\Gamma)$ inner-product, the induced norm of which is denoted by $\|u\|_{0,\Gamma} := \left(\int_\Gamma u^2\, ds\right)^{1/2}$. The related smallest effective, i.e., smallest positive eigenvalues of S^h_{FEM} and S^h_{BEM} are

$$\widehat{\lambda}^h_{\mathrm{FEM}} := \min_{v^h \in V^h \setminus \{0\}} \frac{\langle S^h_{\mathrm{FEM}}(v^h), v^h \rangle}{\|v^h\|^2_{0,\Gamma}}, \quad \widehat{\lambda}^h_{\mathrm{BEM}} := \min_{v^h \in V^h \setminus \{0\}} \frac{\langle S^h_{\mathrm{BEM}}(v^h), v^h \rangle}{\|v^h\|^2_{0,\Gamma}}.$$

By the variational argument, the continuous as well as discrete harmonic extensions minimize the $H^1(\Omega)$-seminorm, denoted by $|\widetilde{u}|_{1,\Omega} := \left(\int_\Omega |\nabla \widetilde{u}|^2\, dx\right)^{1/2}$, over $\widetilde{V}^h$ and $\widetilde{U}^h$, respectively, hence,

$$\widehat{\lambda}^h_{\mathrm{FEM}} = \min_{\widetilde{v}^h \in \widetilde{V}^h \setminus \{0\}} \frac{|\widetilde{v}^h|^2_{1,\Omega}}{\|\widetilde{v}^h\|^2_{0,\Gamma}}, \quad \widehat{\lambda}^h_{\mathrm{BEM}} = \min_{\widetilde{u}^h \in \widetilde{U}^h \setminus \{0\}} \frac{|\widetilde{u}^h|^2_{1,\Omega}}{\|\widetilde{u}^h\|^2_{0,\Gamma}}. \tag{9}$$

These are Galerkin approximations of the smallest positive eigenvalue of S,

$$\widehat{\lambda} := \min_{\widetilde{u} \in \widetilde{U} \setminus \{0\}} \frac{|\widetilde{u}|^2_{1,\Omega}}{\|\widetilde{u}\|^2_{0,\Gamma}}. \tag{10}$$

The related variational formulation reads to find $\widehat{\lambda} \in \mathbb{R}$ and $\widehat{u} \in \widetilde{U} \setminus \{0\}$:

$$\int_\Omega \nabla \widehat{u} \cdot \nabla \widetilde{v}\, dx = \widehat{\lambda} \int_\Gamma \widehat{u}\, \widetilde{v}\, ds \quad \forall \widetilde{v} \in \widetilde{U}. \tag{11}$$

Lemma 1. *It holds that*

$$\widehat{\lambda}^h_{\mathrm{FEM}} \to \widehat{\lambda} \text{ and } \widehat{\lambda}^h_{\mathrm{BEM}} \to \widehat{\lambda} \text{ as } h \to 0. \tag{12}$$

Proof. We apply the theory of Galerkin approximations to eigenvalue problems presented in [21]. To validate the assumptions of the theory it is straightforward to see that $\widetilde{U}$ is a Hilbert space, the bilinear form on the left-hand-side of (11)

is continuous, symmetric, and $\widehat{U}$-elliptic, the bilinear form on the right-hand-side of (11) is continuous and symmetric, and the spaces $\widetilde{V}^h$ and $\widetilde{U}^h$ are finite-dimensional subspaces of $\widetilde{U}$. Furthemore, the subspaces fulfill the approximation property,

$$\forall \widetilde{v} \in \widetilde{U} : \lim_{h\to 0} \min_{\widetilde{v}^h \in \widetilde{V}^h} \|\widetilde{v} - \widetilde{v}^h\|_{1,\Omega} = 0 \text{ and } \lim_{h\to 0} \min_{\widetilde{u}^h \in \widetilde{U}^h} \|\widetilde{v} - \widetilde{u}^h\|_{1,\Omega} = 0.$$

For this setup it is enough to prove, see case 1) on page 100 of [21], that the solution operator $A : \widetilde{U} \to \widetilde{U}$ defined by

$$\int_\Omega \nabla(A\widetilde{u}) \cdot \nabla \widetilde{v}\, dx = \int_\Gamma \widetilde{u}\, \widetilde{v}\, ds \quad \forall \widetilde{v} \in \widetilde{U} \tag{13}$$

is compact on $\widetilde{U}$. The latter is true since A is compounded of three linear bounded operators, one of which is compact. Namely, A compounds of the trace operator $\gamma : H^1(\Omega) \to H^{1/2}(\Gamma)$, the embedding $H^{1/2}(\Gamma) \to L^2(\Gamma)$, which is by Rellich theorem [22] compact, and of the Riesz mapping, related to (13), from $L^2(\Gamma)$ to $H^1(\Omega)$. This chain of operators preserve $\int_\Gamma \widetilde{u}\, ds = \int_\Gamma A\widetilde{u}\, ds = 0$. □

We are actually interested in proving the convergence of the smallest eigenvalues with respect to the scaled Euclidean inner product $(u^h, v^h)_{h,\Gamma}$. We shall denote the norm by $\|v^h\|_{h,\Gamma} := \left((v^h, v^h)_{h,\Gamma}\right)^{1/2}$. By the variational argument for the Steklov-Poincaré operator, these eigenvalues read as follows:

$$\lambda^h_{\text{FEM}} := \min_{\widetilde{v}^h \in \widetilde{V}^h \setminus \{0\}} \frac{|\widetilde{v}^h|^2_{1,\Omega}}{\|\widetilde{v}^h\|^2_{h,\Gamma}}, \quad \lambda^h_{\text{BEM}} := \min_{\widetilde{u}^h \in \widetilde{U}^h \setminus \{0\}} \frac{|\widetilde{u}^h|^2_{1,\Omega}}{\|\widetilde{u}^h\|^2_{h,\Gamma}}. \tag{14}$$

The following Lemma gives the difference between the norms.

Lemma 2. *For each $v^h \in V^h$, it holds that*

$$\|v^h\|^2_{h,\Gamma} = \|v^h\|^2_{0,\Gamma} + \frac{h^2}{6}|v^h|^2_{1,\Gamma}, \tag{15}$$

where the last term is the $L^2(\Gamma)$-norm of tangential derivatives,

$$|v^h|^2_{1,\Gamma} := \int_\Gamma \left(\frac{dv^h}{dt}\right)^2 ds.$$

Proof. For the continuous piecewise linear function v^h, recalling that $v^h(x_0) = v^h(x_n)$ and the boundary discretization is equidistant with the step-length h, the statement follows from simple calculus. Switching between the sum over

elements γ_i and the sum over nodes x_i we get

$$\begin{aligned}
\|v^h\|_{0,\Gamma}^2 &= \sum_{i=1}^n \int_{\gamma_i} (v^h)^2 \, ds = h \sum_{i=1}^n \int_0^1 \left\{ v^h(x_{i-1})\,(1-t) + v^h(x_i)\,t \right\}^2 dt \\
&= \frac{h}{3} \sum_{i=1}^n \left\{ \left[v^h(x_{i-1})\right]^2 + \left[v^h(x_i)\right]^2 + v^h(x_{i-1})\,v^h(x_i) \right\} \\
&= 2 \cdot \frac{h}{3} \sum_{i=1}^n \left[v^h(x_i)\right]^2 + \frac{h}{3} \sum_{i=1}^n v^h(x_{i-1})\,v^h(x_i) \\
&= h \sum_{i=1}^n \left[v^h(x_i)\right]^2 + \frac{h}{3} \sum_{i=1}^n \left\{ -\frac{\left[v^h(x_{i-1})\right]^2}{2} - \frac{\left[v^h(x_i)\right]^2}{2} + \frac{2 v^h(x_{i-1})\,v^h(x_i)}{2} \right\} \\
&= \underbrace{h \sum_{i=1}^n \left[v^h(x_i)\right]^2}_{=\|v^h\|_{h,\Gamma}^2} - \frac{h^2}{6} \underbrace{h \sum_{i=1}^n \left[\frac{v^h(x_i) - v^h(x_{i-1})}{h} \right]^2}_{=|v^h|_{1,\Gamma}^2}.
\end{aligned}$$

□

As a consequence of $\|v^h\|_{h,\Gamma}^2 \geq \|v^h|_{0,\Gamma}^2$:

$$\lambda_{\mathrm{BEM}}^h \leq \widehat{\lambda}_{\mathrm{BEM}}^h \text{ and } \lambda_{\mathrm{FEM}}^h \leq \widehat{\lambda}_{\mathrm{FEM}}^h. \tag{16}$$

Finally, we will need the following inverse inequality.

Lemma 3. *There exists $C > 0$ depending only on Ω such that for all discretizations $\widetilde{U}^h$ and for all eigenfunctions $u_{\mathrm{BEM}}^h \in \widetilde{U}^h$ that are related to the eigenvalue λ_{BEM}^h and that are normalized $\|u_{\mathrm{BEM}}^h\|_{0,\Gamma} = 1$ it holds that*

$$h \left| \widehat{u}_{\mathrm{BEM}}^h \right|_{1,\Gamma}^2 \leq C.$$

Proof. Assume by contradiction that $h \left| u_{\mathrm{BEM}}^h \right|_{1,\Gamma}^2 \to \infty$ as $h \to 0$. We recall the Sobolev-Slobodeckij seminorm,

$$|u|_{1/2,\Gamma}^2 = \int_\Gamma \int_\Gamma \left[\frac{u(x) - u(y)}{|x-y|} \right]^2 ds(y)\, ds(x), \quad u \in H^{1/2}(\Gamma).$$

Obviously,

$$h \left| u_{\mathrm{BEM}}^h \right|_{1,\Gamma}^2 = \sum_{i=1}^n \int_{\gamma_i} \underbrace{\int_{\gamma_i} \left[\frac{u_{\mathrm{BEM}}^h(x) - u_{\mathrm{BEM}}^h(y)}{|x-y|} \right]^2 ds(y)}_{= h \left(\frac{d u_{\mathrm{BEM}}^h}{dt}(x) \right)^2} ds(x) \leq \left| u_{\mathrm{BEM}}^h \right|_{1/2,\Gamma}^2.$$

By the Poincaré inequality and the trace theorem there exists $c > 0$ depending only on Ω such that

$$\left| u_{\mathrm{BEM}}^h \right|_{1,\Omega}^2 \geq c \left(\left\| u_{\mathrm{BEM}}^h \right\|_{0,\Gamma}^2 + \left| u_{\mathrm{BEM}}^h \right|_{1/2,\Gamma}^2 \right).$$

We arrive at the conclusion that

$$\lambda^h_{\mathrm{BEM}} = \frac{|u^h_{\mathrm{BEM}}|^2_{1,\Omega}}{\|u^h_{\mathrm{BEM}}\|^2_{h,\Gamma}} \geq c\, \frac{\overbrace{\|u^h_{\mathrm{BEM}}|^2_{0,\Gamma}}^{=1} + \overbrace{|u^h_{\mathrm{BEM}}|^2_{1/2,\Gamma}}^{\geq h|u^h_{\mathrm{BEM}}|^2_{1,\Gamma}}}{\underbrace{\|u^h_{\mathrm{BEM}}|^2_{0,\Gamma}}_{=1} + \frac{h}{6} h|u^h_{\mathrm{BEM}}|^2_{1,\Gamma}} \geq c\, \frac{\frac{1}{h|u^h_{\mathrm{BEM}}|^2_{1,\Gamma}} + 1}{\frac{1}{h|u^h_{\mathrm{BEM}}|^2_{1,\Gamma}} + \frac{h}{6}} \to \infty,$$

which is a contradiction with $\lambda^h_{\mathrm{BEM}} \leq \widehat{\lambda}^h_{\mathrm{BEM}} \to \widehat{\lambda} \in \mathbb{R}$. □

We get the final result for the lower bound.

Theorem 1. *It holds that*

$$\frac{\lambda^h_{\mathrm{FEM}}}{\lambda^h_{\mathrm{BEM}}} \to 1 \text{ as } h \to 0.$$

Proof. First, we prove the convergence of eigenvalues, $\widehat{\lambda}^h_{\mathrm{BEM}} - \lambda^h_{\mathrm{BEM}} \to 0$,

$$\begin{aligned}
0 &\overset{(16)}{\leq} \widehat{\lambda}^h_{\mathrm{BEM}} - \lambda^h_{\mathrm{BEM}} \overset{(9),(14)}{=} \frac{|\widehat{u}^h_{\mathrm{BEM}}|^2_{1,\Omega}}{\|\widehat{u}^h_{\mathrm{BEM}}\|^2_{0,\Gamma}} - \frac{|u^h_{\mathrm{BEM}}|^2_{1,\Omega}}{\|u^h_{\mathrm{BEM}}\|^2_{h,\Gamma}} \\
&\overset{(9)}{\leq} \frac{|u^h_{\mathrm{BEM}}|^2_{1,\Omega}}{\|u^h_{\mathrm{BEM}}\|^2_{0,\Gamma}} - \frac{|u^h_{\mathrm{BEM}}|^2_{1,\Omega}}{\|u^h_{\mathrm{BEM}}\|^2_{h,\Gamma}} \\
&\overset{(15)}{=} \frac{|u^h_{\mathrm{BEM}}|^2_{1,\Omega} \left(\|u^h_{\mathrm{BEM}}\|^2_{0,\Gamma} + \frac{h^2}{6}\|u^h_{\mathrm{BEM}}\|^2_{1,\Gamma}\right) - |u^h_{\mathrm{BEM}}|^2_{1,\Omega}\, \|u^h_{\mathrm{BEM}}\|^2_{0,\Gamma}}{\|u^h_{\mathrm{BEM}}\|^2_{0,\Gamma}\, \|u^h_{\mathrm{BEM}}\|^2_{h,\Gamma}} \qquad (17) \\
&= \underbrace{\frac{|u^h_{\mathrm{BEM}}|^2_{1,\Omega}}{\|u^h_{\mathrm{BEM}}\|^2_{h,\Gamma}}}_{=\lambda^h_{\mathrm{BEM}} \leq \widehat{\lambda}^h_{\mathrm{BEM}} \to \widehat{\lambda}} \cdot \underbrace{\frac{h}{6}}_{\to 0} \cdot \underbrace{\frac{h|u^h_{\mathrm{BEM}}|^2_{1,\Gamma}}{\|u^h_{\mathrm{BEM}}\|^2_{0,\Gamma}}}_{\leq C} \to 0 \text{ as } h \to 0.
\end{aligned}$$

Now the assertion follows,

$$1 \overset{\widetilde{V}^h \subset \widetilde{U}^h}{\geq} \frac{\lambda^h_{\mathrm{BEM}}}{\lambda^h_{\mathrm{FEM}}} \overset{(16)}{\geq} \frac{\lambda^h_{\mathrm{BEM}}}{\widehat{\lambda}^h_{\mathrm{FEM}}} = \frac{\left(\lambda^h_{\mathrm{BEM}} - \widehat{\lambda}^h_{\mathrm{BEM}}\right) + \widehat{\lambda}^h_{\mathrm{BEM}}}{\widehat{\lambda}^h_{\mathrm{FEM}}} \overset{(17),(12)}{\to} \frac{0 + \widehat{\lambda}}{\widehat{\lambda}} = 1$$

□

Note that by the scaling argument,

$$|\widetilde{u}|^2_{1,\Omega} = |\widetilde{u}_1|^2_{1,\Omega_1},$$

where $\Omega := (0, H)^2$, $\Omega_1 := (0, 1)^2$, $\widetilde{u}(x) = \widetilde{u}_1(x_1)$ for $x \in \Omega$ and $x_1 \in \Omega_1$, the eigenvalue ratio $\frac{\lambda^h_{\mathrm{FEM}}}{\lambda^h_{\mathrm{BEM}}}$ is independent of H.

3.2 Upper Bounds

Lemma 4. *Let $T \subset \mathbb{R}^2$ be an isosceles right triangle with vertices a, b, c and the right angle at the vertex c. Then for any function $u : \mathbb{R}^2 \to \mathbb{R}$ which is linear on the triangle T, it holds that*

$$\int_T |\nabla u|^2 \, dx = \frac{1}{2} \left[\big(u(a) - u(c)\big)^2 + \big(u(b) - u(c)\big)^2 \right].$$

Proof. Without loss of generality assume that $a = (h, 0)$, $b = (0, h)$ and $c = (0, 0)$. Since the function u is linear on T, it clearly holds that

$$u(x, y) = u(c) + \frac{u(a) - u(c)}{h} x + \frac{u(b) - u(c)}{h} y.$$

Therefore

$$|\nabla u|^2 = \left(\frac{\partial u}{\partial x}\right)^2 + \left(\frac{\partial u}{\partial y}\right)^2 = \frac{1}{h^2} \left[\big(u(a) - u(c)\big)^2 + \big(u(b) - u(c)\big)^2 \right].$$

Hence, the lemma immediately follows because the area of the triangle T equals $\frac{h^2}{2}$. □

Lemma 5. *Let $\frac{H}{h} \in \mathbb{N}$. Then for all $v^h \in V^h$ it holds that*

$$\langle S^h_{\mathrm{FEM}}(v^h), v^h \rangle \leq 3 \sum_{i=1}^{n} \big[v^h(x_i)\big]^2, \tag{18}$$

i.e., $h\Lambda^h_{\mathrm{FEM}} \leq 3$.

Proof. Let $v^h \in V^h$ be given and assume the function $\widetilde{v}^h \in \widetilde{V}^h$ be such that v^h and $\widetilde{v}^h$ coincide on Γ and $\widetilde{v}^h$ vanishes on $\Omega_0 := (h, H - h)^2$. By definition (6) of S^h_{FEM} and by the definition and properties of the discrete harmonic extension, we get

$$\langle S^h_{\mathrm{FEM}}(v^h), v^h \rangle = \int_\Omega \left|\nabla \left(\mathcal{H}^h(v^h)\right)\right|^2 dx \leq \int_\Omega \left|\nabla \widetilde{v}^h\right|^2 dx = \int_{\Omega_1} \left|\nabla \widetilde{v}^h\right|^2 dx \tag{19}$$

with $\Omega_1 := \Omega \setminus \overline{\Omega_0}$; see Fig. 2. Now let R be one of the squares belonging to Ω_1 as depicted in Fig. 2 with the side-length h and vertices at the discretization points. If this square does not lie in the corner of Ω, then only two of its vertices, which we denote by a and b, lie on Γ. At the two remaining vertices, the function $\widetilde{v}^h$ vanishes. By Lemma 4 and the elementary inequality

$$(\alpha - \beta)^2 \leq 2(\alpha^2 + \beta^2), \tag{20}$$

it follows that

$$\begin{aligned} \int_R \left|\nabla \widetilde{v}^h\right|^2 dx &= \frac{1}{2} \left(\big[\widetilde{v}^h(a) - \widetilde{v}^h(b)\big]^2 + \big[\widetilde{v}^h(a)\big]^2 + \big[\widetilde{v}^h(b)\big]^2 \right) \\ &\leq \frac{3}{2} \left(\big[\widetilde{v}^h(a)\big]^2 + \big[\widetilde{v}^h(b)\big]^2 \right) = \frac{3}{2} \left(\big[v^h(a)\big]^2 + \big[v^h(b)\big]^2 \right). \end{aligned}$$

If the square R appears in a corner of the domain Ω, then three of its vertices lie on Γ. Let us denote these vertices by a, b and c so that the vertex c is a corner of the domain Ω. At the fourth vertex of R, the function $\widetilde{v}^h$ vanishes. Once more, we use Lemma 4 and inequality (20) to get

$$\begin{aligned}
&\int_R \left|\nabla \widetilde{v}^h\right|^2 dx \\
&= \frac{1}{2}\left(\left[\widetilde{v}^h(a)-\widetilde{v}^h(c)\right]^2+\left[\widetilde{v}^h(c)-\widetilde{v}^h(b)\right]^2+\left[\widetilde{v}^h(a)\right]^2+\left[\widetilde{v}^h(b)\right]^2\right) \\
&\le \frac{1}{2}\left(2\left[\widetilde{v}^h(a)\right]^2+2\left[\widetilde{v}^h(c)\right]^2+2\left[\widetilde{v}^h(c)\right]^2+2\left[\widetilde{v}^h(b)\right]^2+\left[\widetilde{v}^h(a)\right]^2+\left[\widetilde{v}^h(b)\right]^2\right) \\
&= \frac{3}{2}\left(\left[\widetilde{v}^h(a)\right]^2+\left[\widetilde{v}^h(b)\right]^2\right)+2\left[\widetilde{v}^h(c)\right]^2=\frac{3}{2}\left(\left[v^h(a)\right]^2+\left[v^h(b)\right]^2\right)+2\left[v^h(c)\right]^2.
\end{aligned}$$

Integral $\int_{\Omega_1}\left|\nabla \widetilde{v}^h\right|^2 dx$ can be expressed as a sum of integrals over the individual squares of the side-length h. However, notice that every boundary non-corner vertex (in the above estimates, we denoted such vertices by a and b) is a common vertex of two squares; therefore, we have to count it twice, while the corner nodes (denoted by c) only once. From these considerations, we immediately get the inequality

$$\int_{\Omega_1}\left|\nabla \widetilde{v}^h\right|^2 dx \le 3\sum_{i=1}^{n}\left[v^h(x_i)\right]^2.$$

Combining the latter with (19) we obtain required inequality (18). □

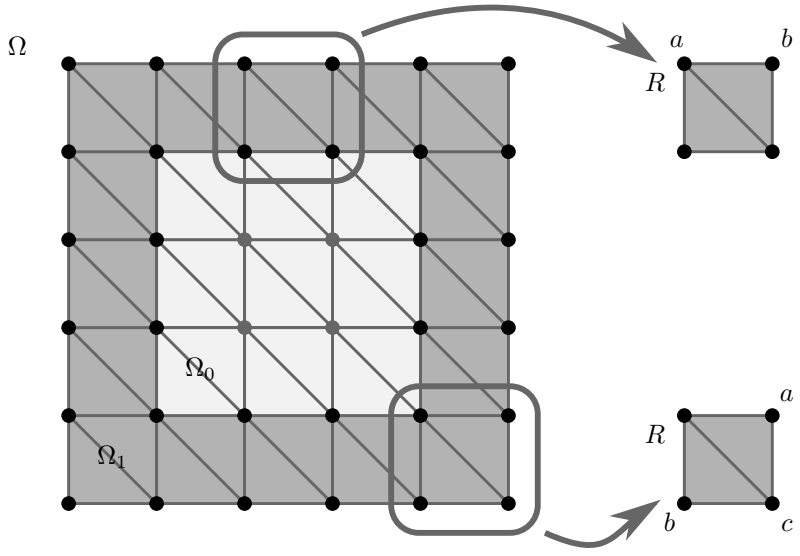

Figure 2: Domains Ω_0 and Ω_1 and two types of squares R.

The following lemma shows that the constant 3 from Lemma 5 cannot be improved much.

Lemma 6. *For all $h \in \mathbb{R}^+$ satisfying $4 \leq \frac{H}{h} \in \mathbb{N}$ it holds that*

$$h\Lambda^h_{\mathrm{FEM}} \geq \frac{\frac{48}{17}\frac{H}{h} - \frac{241}{68}}{\frac{H}{h} - 1} \to \frac{48}{17} \doteq 2.82 \quad \textit{for } h \to 0.$$

Proof. Let us consider a function w^h which is continuous and piecewise linear on Γ and at the corresponding boundary vertices (except the corner ones), it alternately attains the values $+1$ and -1; see Fig. 3. At the corner vertices, we assume w^h vanishes; see Fig. 3. Such a function certainly satisfies the condition

$$\int_\Gamma w^h \, ds = 0,$$

implying that $w^h \in V^h$.

Further, let us consider its discrete harmonic extension $\widetilde{w}^h := \mathcal{H}^h(w^h) \in \widetilde{V}^h$. Then it holds that

$$\langle S^h_{\mathrm{FEM}}(w^h), w^h \rangle = \int_\Omega \left|\nabla \widetilde{w}^h\right|^2 dx \geq \int_{\Omega_2} \left|\nabla \widetilde{w}^h\right|^2 dx,$$

where $\Omega_2 := \Omega \setminus \overline{(2h, H-2h)^2}$; see Fig. 3. For the sake of simplicity, let the numbers α, β, γ, and δ together with $+1$, -1, and 0 represent function values of $\widetilde{w}^h$ at the corresponding vertices; see Fig. 3.

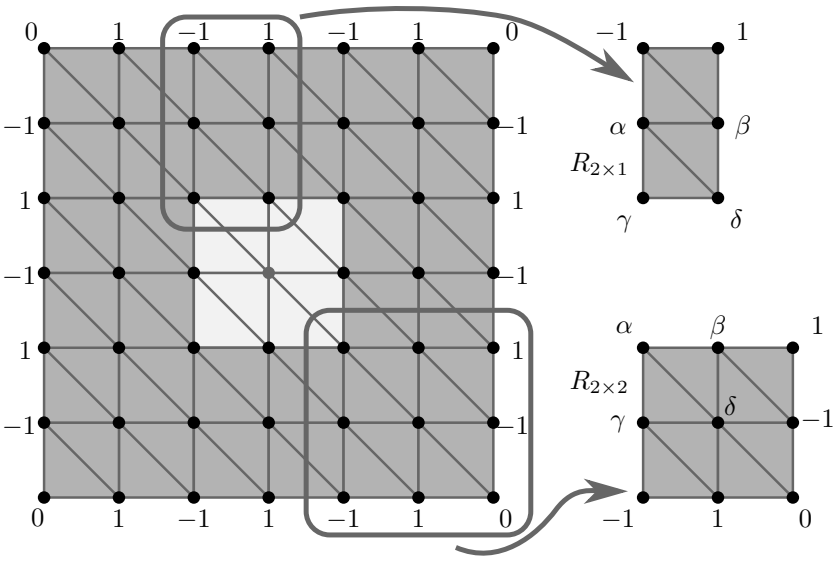

Figure 3: Function w^h and its harmonic extension $\widetilde{w}^h$ on Ω_2.

Using Lemma 4 we get

$$\int_{R_{2\times 1}} \left|\nabla \widetilde{w}^h\right|^2 \, dx = \frac{1}{2}\left[4 + (\beta-1)^2 + (\alpha-\beta)^2 + (\alpha+1)^2 \right.$$
$$\left. +(\alpha-\beta)^2 + (\beta-\delta)^2 + (\gamma-\delta)^2 + (\alpha-\gamma)^2\right].$$

The right-hand side of the latter equality can be viewed as a quadratic function of the variables $\alpha, \beta, \gamma, \delta$ and by a standard calculation, we obtain that the minimum value of this function equals $\frac{48}{17}$. Thus, we have

$$\int_{R_{2\times 1}} \left|\nabla \widetilde{w}^h\right|^2 \, dx \geq \frac{48}{17}.$$

Similarly, we get

$$\begin{aligned}\int_{R_{2\times 2}} \left|\nabla \widetilde{w}^h\right|^2 \, dx = \frac{1}{2}\big[&(\alpha-\beta)^2 + (\beta-\delta)^2 + (\gamma-\delta)^2 + (\alpha-\gamma)^2 \\ &+ (\beta-1)^2 + 4 + (\delta+1)^2 + (\beta-\delta)^2 \\ &+ (\gamma-\delta)^2 + (\delta-1)^2 + 4 + (\gamma+1)^2 \\ &+(\delta+1)^2 + 1 + 1 + (\delta-1)^2\big].\end{aligned}$$

The right-hand side of the latter equality can again be viewed as a quadratic function of the four variables, the minimum value of which equals $\frac{31}{4}$. This means that

$$\int_{R_{2\times 2}} \left|\nabla \widetilde{w}^h\right|^2 \, dx \geq \frac{31}{4}.$$

The following is straightforward since the domain Ω_2 can be assembled out of $4\left(\frac{H}{h}-4\right)$ shapes of $R_{2\times 1}$-type and from 4 shapes of $R_{2\times 2}$-type. Altogether we get

$$\langle S^h_{\mathrm{FEM}}(w^h), w^h\rangle \geq \int_{\Omega_2} \left|\nabla \widetilde{w}^h\right|^2 \, dx \geq 4\left(\frac{H}{h}-4\right)\cdot\frac{48}{17} + 4\cdot\frac{31}{4}.$$

Furthermore, it is clear that

$$\sum_{i=1}^n \left[w^h(x_i)\right]^2 = 4\left(\frac{H}{h}-1\right).$$

By the definition of Λ^h_{FEM} we now get

$$h\Lambda^h_{\mathrm{FEM}} \geq \frac{\langle S^h_{\mathrm{FEM}}(w^h), w^h\rangle}{\sum_{i=1}^n \left[w^h(x_i)\right]^2} \geq \frac{4\left(\frac{H}{h}-4\right)\cdot\frac{48}{17} + 4\cdot\frac{31}{4}}{4\left(\frac{H}{h}-1\right)} = \frac{\frac{48}{17}\frac{H}{h} - \frac{241}{68}}{\frac{H}{h}-1}.$$

□

Lemma 7. *Let $3 \leq \frac{H}{h} \in \mathbb{N}$. Then for all $v^h \in V^h$ it holds that*

$$\langle S^h_{\mathrm{BEM}}(v^h), v^h\rangle \leq \frac{3}{2}\sum_{i=1}^n \left[v^h(x_i)\right]^2, \tag{21}$$

i.e., $h\Lambda^h_{\mathrm{BEM}} \leq \frac{3}{2}$.

Proof. Let $v^h \in V^h$ be given. Similarly to the proof of Lemma 5, we consider an arbitrary function $\widetilde{u}^h \in \widetilde{U}^h \cap C(\overline{\Omega})$ satisfying $\widetilde{u}^h|_\Gamma = v^h$ and vanishing on $\Omega_0 = (h, H-h)^2$. By definition (7) of S^h_{BEM} and by the definition and properties of the harmonic extension, we get

$$\langle S^h_{\mathrm{BEM}}(v^h), v^h\rangle = \int_\Omega \left|\nabla\left(\mathcal{H}(v^h)\right)\right|^2 dx \le \int_\Omega \left|\nabla\widetilde{u}^h\right|^2 dx = \int_{\Omega_1} \left|\nabla\widetilde{u}^h\right|^2 dx, \quad (22)$$

where $\Omega_1 := \Omega \setminus \overline{\Omega_0}$ (like in the proof of Lemma 5). However, now the function $\widetilde{u}^h$ does not need to be piecewise linear. Let us define the function $\widetilde{u}^h$ (satisfying the above properties) as

$$\widetilde{u}^h(x,y) := \begin{cases} v^h(x,0)\left(\frac{h-y}{h}\right)^2 & \text{for } (x,y) \in (h, H-h)\times(0,h), \\ v^h(H,y)\left(\frac{H-h-x}{h}\right)^2 & \text{for } (x,y) \in (H-h,H)\times(h,H-h), \\ v^h(x,H)\left(\frac{H-h-y}{h}\right)^2 & \text{for } (x,y) \in (h,H-h)\times(H-h,H), \\ v^h(0,y)\left(\frac{h-x}{h}\right)^2 & \text{for } (x,y) \in (0,h)\times(h,H-h). \end{cases}$$

Since we need $\widetilde{u}^h(x,y) = 0$ for $(x,y) \in \Omega_0$, it remains to define the function $\widetilde{u}^h$ in the corner squares of the domain Ω. For instance, consider the left lower corner square $R := (0,h)^2$ (we would proceed analogously for the cases of the three remaining corner squares) and denote the function values of v^h at its three vertices $(h,0)$, $(0,h)$, and $(0,0)$ by α, β, and γ, respectively. In view of what was said above, it holds that $\widetilde{u}^h(h,h) = 0$ since $(h,h) \in \overline{\Omega_0}$. Let us divide the square $R = (0,h)^2$ into two triangles

$$T_1 := \{(x,y) \in \mathbb{R}^2 : 0 < y < x < h\},$$
$$T_2 := \{(x,y) \in \mathbb{R}^2 : 0 < x < y < h\}$$

and define

$$\widetilde{u}^h(x,y) := \begin{cases} \alpha\left(\frac{h-y}{h}\right)^2 + \frac{h-x}{h}\left[\gamma\left(\frac{h-y}{h}\right)^{\frac{3}{2}} - \alpha\left(\frac{h-y}{h}\right)\right] & \text{for } (x,y) \in T_1, \\ \beta\left(\frac{h-x}{h}\right)^2 + \frac{h-y}{h}\left[\gamma\left(\frac{h-x}{h}\right)^{\frac{3}{2}} - \beta\left(\frac{h-x}{h}\right)\right] & \text{for } (x,y) \in T_2. \end{cases}$$

Now let us consider one of the squares R with the side-length h that belongs to Ω_1, and its vertices are at the discretization points. If this square does not lie in the corner of Ω, only two of its vertices lie on Γ. Let us denote the function values of $\widetilde{u}^h$ at these vertices by σ and τ. Then, using the definition of the function $\widetilde{u}^h$, we can calculate directly that

$$\int_R \left|\nabla\widetilde{u}^h\right|^2 dx = \frac{29}{45}\sigma^2 + \frac{2}{45}\sigma\tau + \frac{29}{45}\tau^2 \le \frac{2}{3}\left(\sigma^2+\tau^2\right).$$

The last inequality is obvious after removing the fractions. If the square R is placed in the corner of Ω, e.g., $R = (0,h)^2$, then

$$\int_R \left|\nabla\widetilde{u}^h\right|^2 dx = \frac{5}{6}\left(\alpha^2+\beta^2\right) + \frac{7}{10}\gamma^2.$$

If we recall (same as in Lemma 5) that every boundary non-corner vertex always appears in two adjacent squares while the corner vertex only in a single (corner) one, we obtain (by summing over all the squares contained in Ω_1) the inequality

$$\int_{\Omega_1} \left|\nabla \widetilde{u}^h\right|^2 \, dx \leq c \sum_{i=1}^{n} \left[v^h(x_i)\right]^2,$$

where

$$c := \max\left\{2 \cdot \frac{2}{3}, \frac{2}{3} + \frac{5}{6}, \frac{7}{10}\right\} = \frac{3}{2}.$$

Because, provided $\frac{H}{h} \geq 3$, two adjacent squares cannot both be corner. From (22), we immediately get the required inequality. □

To conclude, Lemmas 6 and 7 yield the following theorem.

Theorem 2. *For all $h > 0$ satisfying $4 \leq \frac{H}{h} \in \mathbb{N}$ it holds that*

$$\frac{\Lambda^h_{\mathrm{FEM}}}{\Lambda^h_{\mathrm{BEM}}} \geq \frac{2}{3} \frac{\frac{48}{17}\frac{H}{h} - \frac{241}{68}}{\frac{H}{h} - 1} \to \frac{32}{17} \doteq 1.88 \text{ as } h \to 0.$$

4 Numerical Experiments

To test the effect of better conditioning of the boundary stiffness matrices obtained by the boundary element method as compared with their finite element counterpart, we implemented TFETI, TBETI and their hybrid versions H-TFETI-DP and H-TBETI-DP into Matlab and into our in-house PERMON package [25]. We carried out the numerical experiments to illustrate the spectral properties and to demonstrate the performance of H-TFETI-DP and H-TBETI-DP on linear problems.

4.1 Spectral properties of TFETI and TBETI

In Table 1, we report on spectral bounds of $\mathsf{S}^h_{\mathrm{FEM}}$, $\mathsf{S}^h_{\mathrm{BEM}}$, and numbers of conjugate gradient (CG) iterations for required relative tolerance 10^{-8}. Note that the numerical realization of $\mathsf{S}^h_{\mathrm{BEM}}$ introduces another approximation error. The numerical realization employs the single-layer operator $\mathcal{V}^h$, the double-layer operator $\mathcal{K}^h$, the hypersingular operator $\mathcal{D}^h$, and a Gramm matrix $\mathcal{M}^h$ as follows:

$$\widetilde{\mathsf{S}}^h_{\mathrm{BEM}} := \mathcal{D}^h + \left((1/2)\mathcal{M}^h + \mathcal{K}^h\right)^T \left(\mathcal{V}^h\right)^{-1} \left((1/2)\mathcal{M}^h + \mathcal{K}^h\right).$$

We refer to [23] for the details. In Table 1, we approximate $\mathsf{S}^h_{\mathrm{BEM}}$ using the interpolation $I_h^{h/8} : V^h \to V^{h/8}$ as follows:

$$\mathsf{S}^h_{\mathrm{BEM}} \approx (I_h^{h/8})^T \widetilde{\mathsf{S}}^{h/8}_{\mathrm{BEM}} I_h^{h/8}.$$

The second and third column of Table 1 depict the convergence ratio of the smallest eigenvalues for $\widetilde{\mathsf{S}}^h_{\mathrm{BEM}}$ and $\mathsf{S}^h_{\mathrm{BEM}}$, respectively. We can see that that according to Theorem 1 the ratios converge from below to 1. The fourth column compares the computed largest eigenvalue of $\mathsf{S}^h_{\mathrm{FEM}}$ to the theory. In columns five and six, the largest eigenvalues of $\widetilde{\mathsf{S}}^h_{\mathrm{BEM}}$ and $\mathsf{S}^h_{\mathrm{BEM}}$ are depicted. According to Lemma 7 they are below 1.5. In column seven, the final ratio of the condition numbers is displayed and it is always better than the predicted theoretical asymptotics 1.88. Finally, according to the typical behaviour of the CG method, the ratio between the CG iterations with $\mathsf{S}^h_{\mathrm{FEM}}$ and $\mathsf{S}^h_{\mathrm{BEM}}$ is proportional to the square root of the ratio of the condition numbers (column seven).

$\frac{H}{h}$	$\frac{\widetilde{\lambda}^h_{\mathrm{BEM}}}{\lambda^h_{\mathrm{FEM}}}$	$\frac{\lambda^h_{\mathrm{BEM}}}{\lambda^h_{\mathrm{FEM}}}$	Λ^h_{FEM}(theory)	$\widetilde{\Lambda}^h_{\mathrm{BEM}}$	Λ^h_{BEM}	$\frac{\overline{\kappa}(\mathsf{S}^h_{\mathrm{FEM}})}{\overline{\kappa}(\widetilde{\mathsf{S}}^h_{\mathrm{BEM}})}$	CG iters
4	0.9663	0.9716	2.6051(2.5833)	1.3152	1.3827	1.9140	24/19
8	0.9926	0.9929	2.7600(2.7206)	1.2606	1.3487	2.1732	33/24
16	0.9982	0.9982	2.8097(2.7755)	1.2569	1.3483	2.2314	45/32
32	0.9996	0.9996	2.8235(2.8003)	1.2569	1.3483	2.2454	45/29

Table 1: Spectral properties of subdomains' Schur complement matrices arising in TFETI/TBETI.

The results in Table 1 agree with the theory presented in Sect. 3. It is seen that the BEM discretization is superior to the FEM discretization regarding the regular condition numbers and, therefore, the numbers of CG iterations.

4.2 H-TFETI-DP and H-TBETI-DP performance comparison

To illustrate the performance of H-TFETI-DP and H-TBETI-DP, we decomposed the rectangular domain $\Omega := (0,2)\times(0,1)$ of the membrane into $64\times 32 = 2048$ square subdomains discretized by 200×200 degrees of freedom each. The subdomains were interconnected into $m\times m$ clusters, $m\in\{2,4\}$. The primal dimension of the resulting FEM discretized problem was 81,920,000, in case of the BEM discretization the primal dimension was 1,638,400 and the dual one in both cases was 810,432. We allocated each cluster one computational core. Numbers of required CG iterations with relative tolerance 10^{-6} are reported in Table 2.

m	number of cores	CG iters
2	512	196/100
4	128	255/128

Table 2: Performance of H-TFETI-DP/H-TBETI-DP with $m\times m$ clusters.

5 Conclusion and Comments

Though it is well-known that the Schur complement of the finite element stiffness matrix with respect to the interior variables is spectrally equivalent to the boundary stiffness matrix obtained by the boundary element method, we proved that the conditioning of the latter matrix is essentially better. The theoretical estimate has also been confirmed by numerical experiments. To demonstrate the effect on practical computation, we discretized an academic linear benchmark by both finite element and boundary element methods and resolved it by the hybrid FETI and hybrid BETI domain decomposition methods. These experiments indicate that the hybrid BETI method can be a competitive alternative to the solution of huge problems such as those considered in Mohr et al. [27]. The result is especially important for the solution of huge variational inequalities (see Dostál et al. [20]).

6 Acknowledgments

The work was partially supported by project SGS No. SP2023/067, VSB-Technical University of Ostrava, Czech Republic. This work was also supported by the Ministry of Education, Youth, and Sports of the Czech Republic through the e-INFRA CZ (ID:90254). The fifth and eighth authors were supported by the grant 22-13220S of the Czech Science Foundation (GACR). We acknowledge that the results of this research have been achieved using the DECI resource ARCHER2 based in the UK at EPCC with support from the PRACE aisbl.

References

[1] C. Farhat, F.-X. Roux, A method of Finite Element Tearing and Interconnecting and its parallel solution algorithm, Int. J. Numer. Methods Engng. 32 1205–1227 (1991)

[2] C. Farhat, F.-X. Roux, An unconventional domain decomposition method for an efficient parallel solution of large-scale finite element systems, SIAM J. Sci. Comput. 13, 379–396 (1992)

[3] C. Farhat, J. Mandel, F.-X. Roux, Optimal convergence properties of the FETI domain decomposition method, Comput. Methods Appl. Mech. Eng. 115, 365–385 (1994)

[4] C. Farhat, M. Lesoinne, K. Pierson, A scalable dual-primal domain decomposition method, Numer. Lin. Algebra and Appl. 7, 7–8, 687–714 (2000)

[5] A. Toselli, O.B. Widlund, Domain Decomposition Methods – Algorithms and Theory, Springer Series on Computational Mathematics 34, Springer, Berlin (2005)

[6] C. Pechstein, Finite and Boundary Element Tearing and Interconnecting Solvers for Multiscale Problems, Springer, Heidelberg (2013)

[7] U. Langer, O. Steinbach, Boundary element tearing and interconnecting methods. Computing 71, 205–228 (2003)

[8] A. Klawonn, O. Rheinbach, A hybrid approach to 3-level FETI, Proc. Appl. Math. Mech. (90),1, 10841–10843 (2008)

[9] A. Klawonn, O. Rheinbach, Highly scalable parallel domain decomposition methods with an application to biomechanics, Z. Angew. Math. Mech. (90),1, 5–32 (2010)

[10] A. Klawonn, M. Lanser, O. Rheinbach, Toward extremally scalable nonlinear domain decomposition methods for elliptic partial differential equations, SIAM J. Sci. Comput. (37),6, C667–C696 (2015)

[11] J. Lee, Domain Decomposition Methods for Auxiliary Linear Problems of an Elliptic Variational Inequality, R. Bank et al. (eds.), Domain Decomposition Methods in Science and Engineering XX, Lecture Notes in Computational Science and Engineering 91, 319–326 (2013)

[12] J. Lee, Two domain decomposition methods for auxiliary linear problems for a multibody variational inequality, SIAM J. Sci. Comput. 35,3, 1350–1375 (2013)

[13] Z. Dostál, D. Horák, R. Kučera, Total FETI - an easier implementable variant of the FETI method for numerical solution of elliptic PDE, Commun. Numer. Methods Eng. 22, 1155–1162 (2006)

[14] T. Brzobohatý, Z. Dostál, T. Kozubek, P. Kovář, A. Markopoulos, Cholesky decomposition with fixing nodes to the stable computation of a generalized inverse of the stiffness matrix of a floating structure, Int. J. Numer. Methods Engrg. 88, 5, 493–509 (2011)

[15] Z. Dostál, T. Kozubek, A. Markopoulos, M. Menšík, Cholesky factorization of a positive semidefinite matrix with known kernel, Applied Mathematics and Computation 217, 6067–6077 (2011)

[16] Z. Dostál, D. Horák, T. Brzobohatý, P. Vodstrčil, Bounds on the spectra of Schur complements of large H-TFETI clusters for 2D Laplacian and applications, Numer. Lin. Agebra and Appl., https://doi.org/10.1002/nla.2344 (2020)

[17] Z. Dostál, T. Brzobohatý, O. Vlach, Schur complement spectral bounds for large hybrid FETI-DP clusters and huge three-dimensional scalar problems, J. Numer. Math. 29 (4), 289–306 (2021)

[18] Z. Dostál, T. Brzobohatý, O. Vlach, L. Říha, On the spectrum of Schur complements of 2D elastic clusters joined by rigid edge modes and hybrid domain decomposition, Numer. Math. 152, 41–66 (2022)

[19] Z. Dostál, T. Brzobohatý, O. Vlach, O. Meca, M. Sadowská, Hybrid TFETI domain decomposition with the clusters joined by faces' rigid modes for solving huge 3D elastic problems, Computational Mechanics 71, 333–347 (2023)

[20] Z. Dostál, D. Horák, J. Kružík, T. Brzobohatý, O. Vlach, Highly scalable hybrid domain decomposition method for the solution of huge scalar variational inequalities, Numer. Algorithms 91(2), 773–801 (2022)

[21] J. Descloux, N. Nassif, J. Rappaz, On spectral approximation: Part 1. The problem of convergence, *R.A.I.R.O.* 12(2), 97–112, 1978

[22] S. Sauter, C. Schwab, Boundary Element Methods. Springer (2011)

[23] O. Steinbach, Numerical Approximation Methods for Elliptic Boundary Value Problems. Finite and Boundary Elements. Springer, New York (2008)

[24] Z. Dostál, F. Gomes Neto, S.A. Santos, Solution of contact problems by FETI domain decomposition with natural coarse space projections, Computer Methods in Applied Mechanics and Engineering 190 (2000), 1611-1627.

[25] PERMON – Parallel, Efficient, Robust, Modular, Object-oriented Numerical software toolbox, http://permon.vsb.cz/

[26] Z. Dostál, T. Kozubek, M. Sadowská, V. Vondrák, Scalable Algorithms for Contact Problems, AMM 36, Springer, New York (2016)

[27] M. Mohr, U. Rüde, B. Wohlmuth, H.-P. Bunge, Challenges for Mantle Convection Simulations at the Exa-Scale: Numerics, Algorithmics and Software, p. In Impact of Scientific Computing on Science and Society, P. Neittaanmäki, M.-L. Rantalainen, Springer, Cham, 75–93 (2023)